Validation of superior reference genes in mouse submandibular glands under developmental and functional regeneration states

HUIKAI LIU[1-3*], LIWEN HE[1-3*], QIANYU CHENG[1-3], WENPING LUO[4], TIANYU ZHAO[3] and DEQIN YANG[1-3]

[1]Department of Endodontics, Stomatological Hospital of Chongqing Medical University; [2]Stomatological Hospital of Chongqing Medical University, Chongqing Key Laboratory of Oral Diseases and Biomedical Sciences; [3]Chongqing Municipal Key Laboratory of Oral Biomedical Engineering of Higher Education; [4]Chongqing Key Laboratory of Oral Diseases and Biomedical Sciences, Chongqing 401147, P.R. China

Abstract. Saliva is crucial for lubricating the mouth and aiding in food digestion. However, the occurrence of oral dysfunction, such as xerostomia, dysphagia or oral infection can markedly reduce the quality of life of affected individuals. The major salivary glands include the submandibular gland (SMG), and sublingual and parotid glands; they are the larger glands in mammals that produce the majority of the saliva. The SMG serves as an effective model for the study of branching morphogenesis and functional regeneration. In order to better understand the key dynamic gene expression patterns during salivary gland development and functional regeneration, it is crucial to search for a panel of reliable reference genes. The present study thus aimed to identify superior reference genes to normalize gene expression data in the SMG under states of development and functional regeneration. First, the developmental SMG samples were harvested from mice in the embryonic and post-natal periods. Functional regeneration samples from a ductal ligation/de-ligation model were obtained at several stages. A total of 12 reference genes (*Actb*, *Actg1*, *Ubc*, *Uba1*, *Uba52*, *Ube2c*, *Tuba1a*, *Tuba1b*, *Tubb5*, *H2afy*, *H2afx* and *Gapdh*) from 430 candidates involving tubulin, histone, actin, ubiquitin and GAPDH family members were screened via transcriptome sequencing (RNA-seq) analysis. RT-qPCR (SYBR-Green) and western blot analysis were then used to semi-quantitatively assess gene and protein expression. The stability of expression was evaluated using the ΔCq, geNorm, BestKeeper, NormFinder and RefFinder methods and software. *Actg1* exhibited the highest stability in the SMG developmental stage, while *Tubb5* was recommended as the most stable reference gene for the SMG regenerative stage. In summary, the present study provides evidence-based selections for superior reference genes in the SMG during the stages of development and functional regeneration.

Introduction

Saliva is crucial for maintaining normal oral function, from lubricating food to removing food residues and maintaining the oral microbiome homeostasis (1). Three pairs of major glands, the submandibular gland (SMG), sublingual gland (SLG) and parotid gland, as well as >1,000 minor glands, comprise the majority of the mammalian salivary system. In humans and mice, these major glands are in similar positions and secrete >90% of the total salivary content in the oral cavity (2).

The developmental stages of the SMG have attracted the attention of numerous researchers. This is due to the fact that SMG morphogenesis in mice exhibits a distinct 'bunch of grapes' appearance, which has been recognized as a classical model for studying the branching of organs (3,4). In the developmental stages of the SMG, the processes of gland initiation and branching morphogenesis are similar in both mice and humans. Unlike humans, the SMG in mice has an additional ductal network that joins intercalated and striated ducts, which serves as the primary source of growth-stimulating molecules, such as the epidermal growth factor and nerve growth factor (5,6). The similarities in salivary gland development between mice and humans suggest that the salivary gland research in mice can lay the foundation for its counterpart in humans, but the differences pose certain limitations. The development of the SMG is initiated in the thickened areas

within the oral epithelial at embryonic day (E)11.5 in mice (the pre-bud stage). The SMG then gives rise to the initial bud on E12, which subsequently gives rise to a new bud, leading to extensive branching into the surrounding mandibular mesenchyme during cytodifferentiation, eventually forming the duct lumen on E15 and mature acini on E18 (3,7). In recent decades, key genes and their related signals regulating branch morphogenesis have been identified, including the sex-determining region Y (*Sox2*) and Wnt/β-catenin (8,9). However, accurate and complete gene regulatory network details regarding salivary gland development need to be elucidated using superior reference genes as controls for normalization using reverse transcription-quantitative PCR (RT-qPCR) analysis with SYBR-Green.

The salivary glands are affected by salivary gland tumors, Sjögren's syndrome, duct blockage, or salivary stones, which can lead to long-lasting oral dysfunction in the form of xerostomia, dysphagia, or oral infections, which can markedly reduce the quality of life of patients (10,11). Artificial saliva, oral moisturizers and salivation stimulators are some of the current treatments for salivary dysfunction; however, these measures only alleviate the clinical symptoms and fail to fundamentally repair the damaged tissues of the gland and restore its function (11). Therefore, studies examining novel therapeutic approaches that aim to regenerate the salivary glands and maintain normal salivary secretion are essential for affected patients. Currently, there are three main strategies for restoring salivary gland function: i) The insertion of a therapeutic gene into ductal cells or residual salivary gland acinar cells by retrograde injection of lentivirus as a vector (12); ii) the activation of stem cell proliferation or differentiation in the gland (13); and iii) the elucidation of signaling pathways associated with salivary gland regeneration (12). Among these three approaches, gene therapy allows for the identification of key genes responsible for regulating the regeneration and repair of duct calculus-induced salivary gland fibrosis (14). The silencing of transforming growth factor 1 (*Tgfb1*) or the activation of sonic hedgehog (*Shh*) might restore salivary function (15,16). The ligation/de-ligation of excretory ducts in SMG has previously been verified as an ideal mouse model to study salivary gland injury and functional regeneration (11). In this process, acinar epithelial cells undergo atrophy, apoptosis and subsequently, regeneration from the differentiation of proliferated duct cells and stem/progenitor cells.

The selection of reference genes is dependent on particular physiopathological processes and various experimental conditions (17). The common reference genes in the development and regeneration of the salivary gland include β-actin (*Actb*) and glyceraldehyde-3-phosphate dehydrogenase (*Gapdh*) (18-20). β-actin is a core components of the cytoskeleton, and its expression has been validated in differentiation and cell migration (21-24). *Gapdh* is used as one of the reference genes due to its role in basic metabolic processes in several organisms. However, several studies have found that the expression of *Gapdh* was not always constant and affected by stress response and growth (25-28). Therefore, it is worth seeking reliable reference genes to explore gene regulatory networks during the SMG development and regeneration process.

The present study screened and evaluated the expression stability of 12 candidate reference genes (*Actb, Actg1, Ubc,* *Uba1, Uba52, Ube2c, Tuba1a, Tuba1b, Tubb5, H2afy, H2afx* and *Gapdh*) in the SMG during the developmental and regenerative states using transcriptome sequencing (RNA-seq), RT-qPCR (SYBR-Green) and western blot analysis. The reliability of identified reference genes was further validated by analyzing the expression pattern of recombinant aquaporin 5 (*AQP5*) and keratin 19 (*KRT19*) genes during the SMG developmental stage, using stable and unstable genes for normalization. The findings presented herein may promote further molecular biological research into the development and functional regeneration of the SMG.

Materials and methods

Experimental animals. All animal experiments were approved by the Ethics Committee of Chongqing Medical University College and Use Committee (approval no. 2021062). The Guidelines for the Ethical Review of Laboratory Animal Welfare (GB/T35892-2018, China) were applied in the experiments. The study was conducted according to the guidelines of ARRIVE and AVMA euthanasia 2020, and followed the '3R' principles for the treatment of experimental animals: Replacement, reduction and refinement. In the present study, C57BL/6N mice were obtained from the Laboratory Animal Center of Chongqing Medical University. The plug day discovery is designated as gestation initiation (E0.5). All the mice were housed under environmentally controlled conditions with a room temperature (22±1°C) and humidity (50-55%), and a 12-h light-dark cycle, with free access to water and standard food.

To comprehensively monitor the expression stability of reference genes throughout the SMG developmental period, C57BL/6N mice from the embryo (E14.5, E15.5, E16.5, E17.5 and E18.5) to the post-natal stage [post-natal day (P)0, P7, P14, P28, P56, P84 and P112] were used in the experiments. There were 16 C57BL/6N fetal mice at E14.5 and E15.5, 8 C57BL/6N fetal mice at E16.5 to E18.5, 3 C57BL/6N mice at P0 to P14, and 6 C57BL/6N mice at P28 to P112, half male and female; it should be noted that at the embryo stage and post-natal stage (P0, P7 and P14), the mice are too small to distinguish the sex.

In order to screen expression stability of reference genes in the SMG functional regenerative states, 45 C57BL/6N female mice (8 weeks old, weighing 20 g) were and divided into the 5-day ligation group, 7-day ligation group, 7-day de-ligation group, 14-day de-ligation group and 28-day de-ligation group, for the unilateral ligation of the SMG main duct surgery (n=9/group). The contralateral glands were not duct-ligated and were defined as the sham operation group.

Duct ligation/de-ligation. The unilateral ligation of the SMG main duct was performed as previously described (11). Age-matched 8-week-old C57BL/6N female mice were anesthetized using isoflurane (2-3% for induction and 1.5-2% for maintenance), followed by an incision of ~20 mm in length in the skin of the neck. The left SMG was exposed by a blunt dissection of the skin at the midline of the neck, and the main duct of the SMG was isolated from the surrounding blood vessels and nerves. Surgical sutures were applied for duct ligation and incision closure, and the mice were allowed to

recover. After 7, 14 and 28 days of obstruction, the mice were subjected to SMG de-ligation.

Sample collection. Pregnant C57BL/6N female mice were anesthetized using isoflurane and sacrificed using CO_2 with a 30-70% container volume/min at E14.5, E15.5, E16.5, E17.5 and E18.5. Embryos were washed with cold PBS to remove blood. SMG tissue was isolated with sterile fine forceps under a stereo dissecting microscope (Nikon SMZ645; Nikon Corporation). Similarly, post-natal glands of C57BL/6N mice, female and male, were harvested at P0, P7, P14, P28, P56, P84 and P112 (the mice at P0, P7 and P14 mice were too small to distinguish the sex). The SMG tissue samples from the physiological state were then collected and processed for RT-qPCR with SYBR-Green and western blot analysis. Furthermore, the glands at 5-day ligation, 7-day ligation, 7-day de-ligation, 14-day de-ligation, 28-day de-ligation and the contralateral control samples were excised under terminal anesthesia using isoflurane and sacrificed using CO_2 with a 30-70% container volume/min and processed for RT-qPCR, western blot analysis and histochemical staining analyses.

Histochemical staining. SMG tissues (5-day ligation, 7-day ligation, 7-day de-ligation, 14-day de-ligation, 28-day de-ligation and contralateral controls) were extracted and fixed in 4% (v/v) paraformaldehyde solution at 4˚C for 24 h, dehydrated in a series of alcohols and embedded in paraffin; 5-μm-thick tissue sections were cut using a paraffin microtome (Leica Microsystems GmbH). The tissue morphology was observed using hematoxylin and eosin (H&E) staining and Alcian blue (AB) and periodic acid-Schiff staining (PAS).

H&E staining was performed at room temperature (23-25˚C) as follows: Briefly, the sections were deparaffinized, rehydrated, stained with hematoxylin solution (Chongqing Mengbio Biotechnology Co., Ltd.) for 5 min at room temperature, differentiated in 1% acid alcohol (1% HCl in 70% ethanol), and blued in tap water for 45 min, then stained with eosin solution for 3 min at room temperature. The sections were then dehydrated with graded alcohol, cleared in xylene and mounted on a cover glass.

The SMG tissues were stained using AB-PAS staining kit (G1285, Beijing Solarbio Science & Technology Co., Ltd.) at room temperature (23-25˚C) based on the manufacturer's instructions. The sections were dewaxed, washed and stained with AB for 10-20 min at room temperature, treated with freshly prepared 0.5% periodate solution for 5 min, stained for 10-20 min with Schiff reagent and counterstained with hematoxylin for 1-2 min at room temperature. Finally, Scott blue solution (Beijing Solarbio Science & Technology Co., Ltd.) was used for re-bluing, followed by dehydrate using a series of ethanol, transparent by xylene and sealing with resin.

RNA-seq data analysis, selection of candidate reference gene and primer design. To conduct the systematic analysis of reference genes during the development and functional regeneration of SMG, SMG samples at E13.5, E16.5, P0, P56 and at 5-day ligation were collected. Transcriptome sequencing was performed by Biomarker Technologies (Beijing) Co., Ltd. and Majorbio (Shanghai) Technology Co., Ltd. Total tissue RNA of SMG was extracted using TRIzol® reagent (Invitrogen;

Thermo Fisher Scientific, Inc.) based on the manufacturer's instructions. A total of 1 μg RNA per sample was used as input material for the RNA sample preparations. Using the NEBNext UltraTM RNA Library Prep kit for Illumina (NEB) in accordance with the manufacturer's instructions, sequencing libraries were created and index codes were added to assign sequences to specific samples. Briefly, mRNA was purified from total RNA using poly-T oligo-attached magnetic beads (Illumina, Inc.). Divalent cations were used to carry out fragmentation at an elevated temperature in NEBNext First Strand Synthesis Reaction Buffer (5X). M-MuLV reverse transcriptase and random hexamer primer were used to create first-strand cDNA. Subsequently, DNA Polymerase I and RNase H were used to create second-strand cDNA. Exonuclease/polymerase operations turned the remaining overhangs into blunt ends. NEBNext Adaptors with a hairpin loop structure were ligated to prepare for hybridization after the 3' ends of DNA fragments were adenylated. The library fragments were purified using the AMPure XP technology (Beckman Coulter, Inc.) to select cDNA fragments that were preferably 240 bp in length. The cDNA that had been size-selected and adaptor-ligated was then utilized in 3 μl USER Enzyme (NEB) and heated at 37˚C for 15 min followed by 5 min at 95˚C prior to PCR. PCR was then carried out using Index (X) Primer, universal PCR primers, and Phusion High-Fidelity DNA polymerase. Finally, PCR products were purified using an AMPure XP system (Illumina, Inc.). Following quality inspection and cluster generation, the library preparations were sequenced using the Illumina HiSeq2000 high-throughput sequencing platform (Illumina, Inc.). The final library loading concentration was 2 nmol/l and the loading volume was 10 μl.

The selection of reference genes was based on transcriptome sequencing information of the aforementioned mouse SMG sample. Fragments per kilobase of exon model per million mapped fragments (FPKM) were used as the normalized value to estimate gene expression in the tissue. The annotated genes obtained from transcript information were classified and candidate reference genes were screened out for verification. Specific PCR primers (Table I) were designed using Primer 3.0 (Applied Biosystems; Thermo Fisher Scientific, Inc.) and synthesized by Sangon Biotech Co., Ltd.

RNA isolation and cDNA synthesis. Frozen samples (~20 mg) were ground using a grinding bead homogenizer (Shanghai Jingxin Industrial Development Co., Ltd.). Total tissue RNA of SMG was extracted using TRIzol® reagent (cat. no. 15596018, Invitrogen; Thermo Fisher Scientific, Inc.) based on the manufacturer's instructions. The purity and concentration of the extracted total RNA was examined using a Nanodrop UV 2000 spectrophotometer (cat. no. ND-2000, Thermo Fisher Scientific, Inc.). The genetic integrity of the isolated RNA was further detected using 2% agarose gel electrophoresis. Only the RNA samples with A260/A280 absorbance ratios of 1.8 and 2.2 were used for follow-up cDNA synthesis analyses. A total of 2 μg total RNA was reverse transcribed into cDNA using a reverse transcription reaction kit (18090050, Invitrogen; Thermo Fisher Scientific, Inc.) with a 20 μl system. The reverse transcription reaction involved incubation at 23˚C for 10 min, followed by 10 min at 55˚C. The transcriptor reverse transcriptase enzyme was inactivated by heating to 80˚C for

Table I. Primer sequences and amplification characteristics of the 12 reference genes and two target genes.

Gene/gene accession no.	Gene name (*Mus musculus*)	Gene function	5'-Forward primer-3' (length/Tm/%GC/Self-Comp/Self-3'-Comp.)	5'-Reverse primer-3' (length/Tm/%GC/Self-Comp/Self-3'-Comp.)	Amplicon (length, efficiency, R^2)
Actb/NM_007393.5	Actin, beta	Cytoskeleton	TCTTTGCAGCTCCTTCGTTG (20 bp/58.77°C/50%/4/0)	CGATGGAGGGAATACAGCC (20 bp/59.96°C/60%/2/1)	150 bp, 103%, 0.996
Actg1/NM_001313923.1	Actin, gamma, cytoplasmic 1	Cytoskeleton	GGCTTACACTGCGCTTCTTG (20 bp/59.83°C/55%/4/0)	GCGATTTCTTCTTCCATTGC (20 bp/55.72°C/45%/3/2)	75 bp, 104%, 0.996
Uba1/XM_030251302.1	Ubiquitin-like modifier activating enzyme 1	Coenzyme transport and metabolism	CCTACACTGGGCCTCTTGTC (20 bp/59.75°C/60%/4/2)	ATGACAGAACTCCCCACTC (20 bp/58.72°C/55%/3/0)	104 bp, 109.4%, 0.998
Ubc/NM_019639.4	Ubiquitin C	Post-translational modification, protein turnover, chaperones	AGCCCAGTGTTACCACCAAG (20 bp/59.89°C/55%/6/2)	CTAAGACACCTCCCCATCA (20 bp/58.12°C/55%/3/1)	118 bp, 103.2%, 0.992
Uba52/NM_001348228.1	Ubiquitin A-52 residue ribosomal rotein fusion product 1	Post-translational modification, protein turnover, chaperones	GGTTCCGCTGTCCTCTTTCT (20 bp/59.68°C/55%/2/0)	GCCTTGACATTCTCGATGGT (20 bp/57.97°C/50%/4/2)	133 bp, 96.4%, 0.995
Ube2c/NM_026785.2	Ubiquitin-conjugating enzyme E2C	Post-translational modification, protein turnover, chaperones	CGGCTACAGGCAGGAACTGAT (20 bp/59.82°C/55%/4/3)	CACCCACTTGAACAGGTTGT (20 bp/58.24°C/50%/5/3)	90 bp, 95.9%, 0.997
H2afy/XM_006517258.3	MacroH2A.1 histone	Chromatin structure and dynamics	CACCTGTGTACATGGCTGCT (20 bp/60.32°C/55%/6/1)	TCATTGGCCACAGCTAACAG (20 bp/58.17°C/50%/6/2)	130 bp, 106.2%, 0.999
H2afx/XM_006509995.3	H2A.X variant histone	Chromatin structure and dynamics	ACCACCTCCCTCACAGAAAG (20 bp/58.94°C/55%/2/1)	GGGAGAGGAGGGAAAAGAGAA (20 bp/57.74°C/55%/0/0)	85 bp, 95.6%, 0.992
Tuba1a/NM_011653.2	Tubulin-alpha 1A	Cytoskeleton	CAGGTCTCCAGGGCTTCTTG (20 bp/60.4°C/60%/3/0)	AATCAGAGTGCTCCAGGGTG (20 bp/59.38°C/55%/4/2)	210 bp, 113.9%, 0.992
Tuba1b/NM_011654.2	Tubulin-alpha 1B	Cytoskeleton	CCCGGTGTCTGCTTCTATCT (20 bp/58.88°C/55%/4/0)	CATGTTCCAGGCAGTAGAGC (20 bp/58.34°C/55%/4/2)	135 bp, 92.3%, 0.995
Tubb5/NM_011655.5	Tubulin-beta 5 class I	Cytoskeleton	GGAAATCGTGCACATCCAGG (20 bp/59.27°C/55%/6/3)	GGGGTCGATGCCATGTTCAT (20 bp/60.47°C/55%/5/4)	91 bp, 98.5%, 0.992
Gapdh/NM_001289726.1	Glyceraldehyde-3-phosphate dehydrogenase	Carbohydrate transport and metabolism	GGCTGCCCAGAACATCAT (18 bp/57.33°C/55.56%/5/3)	CGGACACATTGGGGGTAG (18 bp/57.05°C/61.11%/3/0)	122 bp, 109.7%, 0.997
AQP5/NM_009701.4[a]	Aquaporin 5	Carbohydrate transport and metabolism	CTCCGAGCCATCTTCTACGT (20 bp/58.97°C/55%/5/4)	CCAATGGATAAGGCTGGGGA (20 bp/59.15°C/55%/5/0)	245 bp, 108.1%, 0.998
Krt19/NM_008471.3[a]	Keratin 19	Cytoskeleton	GGTTCAGTACGCATTGGGTC (20 bp/58.92°C/55%/5/3)	CAAGTAGGAGGCGAGACGAT (20 bp/58.97°C/55%/2/2)	234 bp, 98%, 0.990

[a]Target genes.

10 min. The generated cDNA products were diluted three-fold with nuclease-free water and stored in a -80˚C freezer for subsequent qPCR analyses.

qPCR. All qPCR reactions were performed in triplicate on an ABI Prism 7500 Real-Time PCR System (Applied Biosystems; Thermo Fisher Scientific, Inc.) using 2X SYBR-Green qPCR Master Mix (Bimake, Houston, TX, USA, http://www.bimake. cn/). A final 20 μl reaction mixture contained 2 μl diluted cDNA template, 0.75 μl of each of the forward and reverse primers, 10 μl of 2X SYBR-Green qPCR Master Mix, and 6.5 μl RNase-free water. The PCR amplification program was as follows: 95˚C for 3 min for initial cDNA hot-start activation, followed by 39 amplification cycles of 95˚C for 10 sec for denaturation, 59˚C for 30 sec for annealing and extension. At the end of amplification, a melting curve analysis was performed at 65 to 95˚C for 5 sec at a heating rate of 0. 5˚C/sec to confirm the specificity of each primer pair. The $2^{-\Delta\Delta Cq}$ method was used as previously reported (29).

Western blot analysis. Frozen gland tissues (~30 mg) were homogenized in ice-cold RIPA lysis buffer (Beyotime Institute of Biotechnology) using a motor-driven tissue grinder. The homogenate was centrifuged at 14,000 x g at 4˚C for 5 min, and the total protein concentration in the supernatant was then quantified using a BCA kit (Beyotime Institute of Biotechnology). All gland protein samples were mixed with 5X loading buffer (Hangzhou Fude Biological Technology Co., Ltd., http://www.fdbio.net/) and immediately denatured by boiling at 100˚C for 10 min. After cooling, the samples were separated on 12% SDS-PAGE, and the protein gel was transferred onto PVDF membranes (MilliporeSigma). The membranes were then blocked (1 h at room temperature) in 5% BSA solution (Beyotime Institute of Biotechnology), and the membranes were incubated overnight at 4˚C with the respective primary antibodies against rabbit anti-ubiquitin (1:400 dilution; cat. no. 20200728, Yurogen Biosystems LLC), rabbit anti-TUBA1B (1:100,000 dilution; cat. no. ab108629, Abcam), rabbit anti-GAPDH (1:1,000 dilution; cat. no. 5174s, Cell Signaling Technology, Inc.) and rabbit anti-ACTB (1:1,000 dilution; cat. no. 8457s, Cell Signaling Technology, Inc.). Subsequently, the membranes were rinsed with TBST (20 mM Tris-HCl, 140 mM NaCl, pH 7.6, 0.1% v/v Tween-20) three times and incubated with HRP-conjugated anti-rabbit IgG secondary antibodies (1:1,500 dilution; cat. no. 7074S, Cell Signaling Technology, Inc.) at room temperature for 1 h. Finally, the blots were incubated with chemiluminescence substrate ECL Western blotting detection reagents (Beyotime Institute of Biotechnology) for 1 min, and the antibody-specific labeling bands were detected using the ChemiDoc™ MP Imaging System (Bio-Rad Laboratories, Inc.) and ImageJ software (v1.8.0; National Institutes of Health) was employed for densitometric results.

Reference gene expression stability. The expression levels of 12 reference genes were determined by the quantification cycle (Cq) value, which was obtained from RT-qPCR. Cq values were converted to relative values using $2^{-\Delta Cq}$, of which ΔCq=the corresponding Cq value-minimum Cq (30). $2^{-\Delta Cq}$ were used for geNorm and the NormFinder software, while BestKeeper analysis was based on raw Cq values. The expression stability of the reference genes was ranked using the ΔCq value and four different types of statistical algorithms software as follows: i) geNorm: The stable value (M) of geNorm software calculated is based on the average pairwise variation between all reference genes tested. M values below the theoretical threshold of 1.5, indicating a stable expression and vice versa (31). ii) NormFinder: The stable value of NormFinder software is based on variation analysis in expression levels, and a lower stable value indicates a high stability (32). iii) BestKeeper: The stable value of BestKeeper is based on the standard deviation (SD) and coefficients of variation (CV), and the most stable reference genes have the lowest CV and SD and vice versa (33). iv) RefFinder: The RefFinder software calculates the geometric mean weight of each gene and the stability rankings based on the analysis of the ΔCq value and the aforementioned three specialized programs and obtains an overall comprehensive ranking (34).

Statistical analysis. All data are expressed as the mean ± standard deviation. Statistical analyses were performed using SPSS 22.0 software (IBM Corp.). The figures were generated using Graphpad Prism 8.0 (GraphPad Software Inc.) and ImageJ software (v1.8.0; National Institutes of Health). The statistical significance of the protein levels was evaluated using one-way ANOVA for repeated measures. A value of P<0.05 was considered to indicate a statistically significant difference.

Results

RNA-Seq reveals candidate reference genes. To observe the morphological changes in the SMG during the developmental stage, SMG samples at E13.5, E16.5, P0, P7 and P14 were collected, and these representative images are illustrated in Fig. 1. At E13.5 (the pre-bud stage), the epithelial bud cleft formation and divides the bud into typically two or three parts. At E16.5 (the microtubule stage), the ductus had abundant branches, numerous acini, and a rudimentary glandular shape, with clearly well-developed lumen seen in terminal buds and putative ductus. After birth, the glands continue to differentiate and grow, with an increase in glandular branching and glandular lobules, and an increase in the number and volume of acinar cells. Furthermore, to conduct a systematic analysis of reference genes during the development of SMG, RNA-Seq of the SMG at E13.5, E16.5, P0 and P56 were performed separately. Excretory duct ligation represented SMG injury and repair (5 days). The raw data for the present study were deposited in the SRA database (accession no. PRJNA856858' to be release on June 30, 2023). RNA-Seq analysis detected >20,000 annotated genes. Utilizing the Pfam, SwissProt, EggNOG and NR databases, 430 genes belonging to the tubulin, histone, actin, ubiquitin and GAPDH family of protein were sorted and classified. These family members were assigned 15 genes (tubulin family), 85 genes (histone family), 22 genes (actin family), 307 genes (ubiquitin family) and 1 gene (GAPDH family). The high FPKM value (>90) of genes with Top4 rank were then selected as potentially the most stably expressed genes for validation. Finally, 12 candidate reference genes were obtained, namely *Tuba1a, Tuba1b, Tubb5, H2afy, H2afx, Actb, Actg1, Ubc, Uba1, Uba52, Ube2c* and *Gapdh*. The
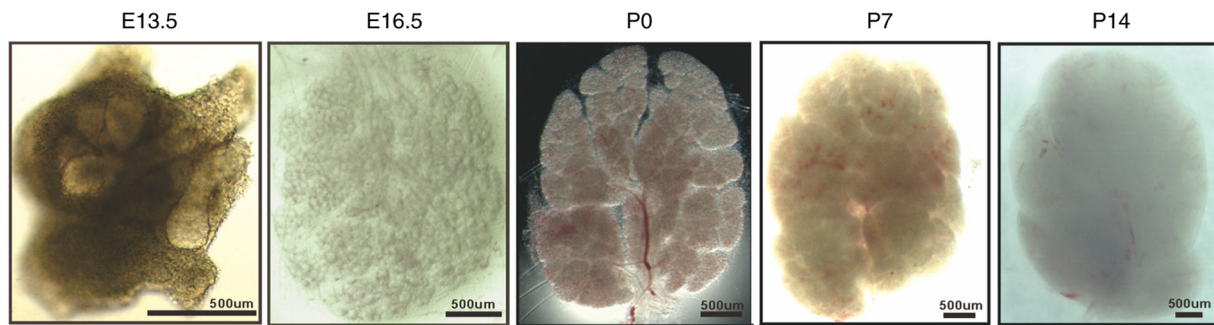
Figure 1. Morphology of the submandibular gland at E13.5, E16.5, P0, P7 and P14. Scale bars, 500 μm. E, embryonic day; P, post-natal day.

heatmap revealed the total RNA expression [Log2(FPKM)] of the 12 candidate reference genes (Fig. 2).

Specificity and amplification efficiency of RT-qPCR primers. Subsequently, total RNA was extracted from the SMG to verify the primer specificity and amplification efficiency of the 12 candidate reference genes and two target genes. First, gland samples were collected from embryonic mice (E14.5, E15.5, E16.5, E17.5 and E18.5), post-natal mice (P0, P7, P14, P28, P56, P84 and P112) and the duct calculus-induced SMG functional regeneration model at 5 and 7 days after ligation and then after 7, 14 and 28 days after de-ligation. RNA purity and concentration were assessed. As shown in Table SI, the A260/A280 ratio ranged from 1.99 to 2.15. The melting curve, amplification efficiency and correlation coefficient (R^2) were confirmed. The melting curves revealed that all candidate reference genes had a single peak without primer, dimers and non-specific PCR products, indicating that each primer pair was highly specific to the targeted region (Fig. S1A). The amplification efficiency varied from 92.3% (*Tuba1b*) to 113.9% (*Tuba1a*) and met the standard for RT-qPCR (Fig. S1B). All linear R^2 values varied from 0.992 to 0.999, indicating a linear association between cDNA levels and Cq values, verifying the reliability of the results. Table I presents the gene accession number, gene name, gene function, primer sequence, amplicon length, product TM (℃), GC (%), self-comp, self-3'-comp, R^2 and efficiency (%) of the 12 candidate reference genes and two target genes. These data indicated that RNA extraction, primer sequences and the amplification procedure were all in accordance with the RT-qPCR assessment.

Candidate reference gene expression profiles. The present study then investigated the expression variability of the 12 candidate reference genes using RT-qPCR. First, gland samples were harvested from embryonic mice (E14.5, E15.5, E16.5, E17.5 and E18.5) and post-natal mice (P0, P7, P14, P28, P56, P84 and P112) and duct calculus-induced SMG functional regeneration model at 5 and 7 days after ligation, and then 7, 14 and 28 days after de-ligation. The Cq values were applied to demonstrate variations among all samples. The contralateral glands without ligation in the same individuals were defined as the sham operation group. The mean Cq values of the 12 candidate reference genes in the SMG development stage, ranging from 17.18 to 23.70 are shown in Fig. 3A; the results suggested that there were relatively large differences in the transcript levels among these reference genes. A low Cq value
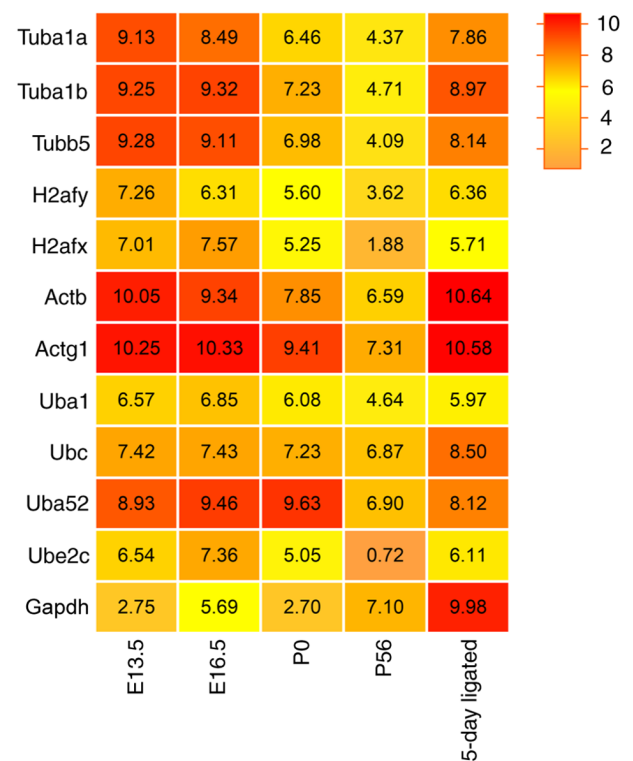

Figure 2. Heatmap of the total RNA expression of the 12 candidate reference genes [Log2(FPKM)] from the RNA-seq analyses in the E13.5, E16.5, P0, P56 and 5-day ligation submandibular gland samples. E, embryonic day; P, post-natal day.

indicates a high gene expression level and vice versa. *Actb* was the most abundant, with Cq values ranging from 13.9 to 19.97, while *Ube2c* was the least abundant transcript, with Cq values ranging from 19.31 to 28.95. To better evaluate these variations, the CV values were calculated. The CV values of the 12 candidate reference genes in all samples from low to high were as follows: 3.98% (*Ubc*), 4.30% (*Uba52*), 6.55% (*Uba1*), 6.73% (*H2afy*), 8.48% (*Gapdh*), 10.73% (*Actg1*), 11.71% (*H2afx*), 12.35% (*Tuba1a*), 12.39% (*Actb*), 13.09% (*Tubb5*), 13.17% (*Tuba1b*) and 14.58% (*Ube2c*) (Fig. 3A).

Similarly, the Cq and CV values in SMG functional regeneration were evaluated. In the sham operation group, the Cq values of the 12 candidate reference genes ranged from 21.43 to 28.79 (Fig. 3B). It was also found that the *Actb* gene expression level was the highest (mean Cq, 21.43), whereas *Ube2c* was the least expressed (mean Cq, 28.79). These results were similar
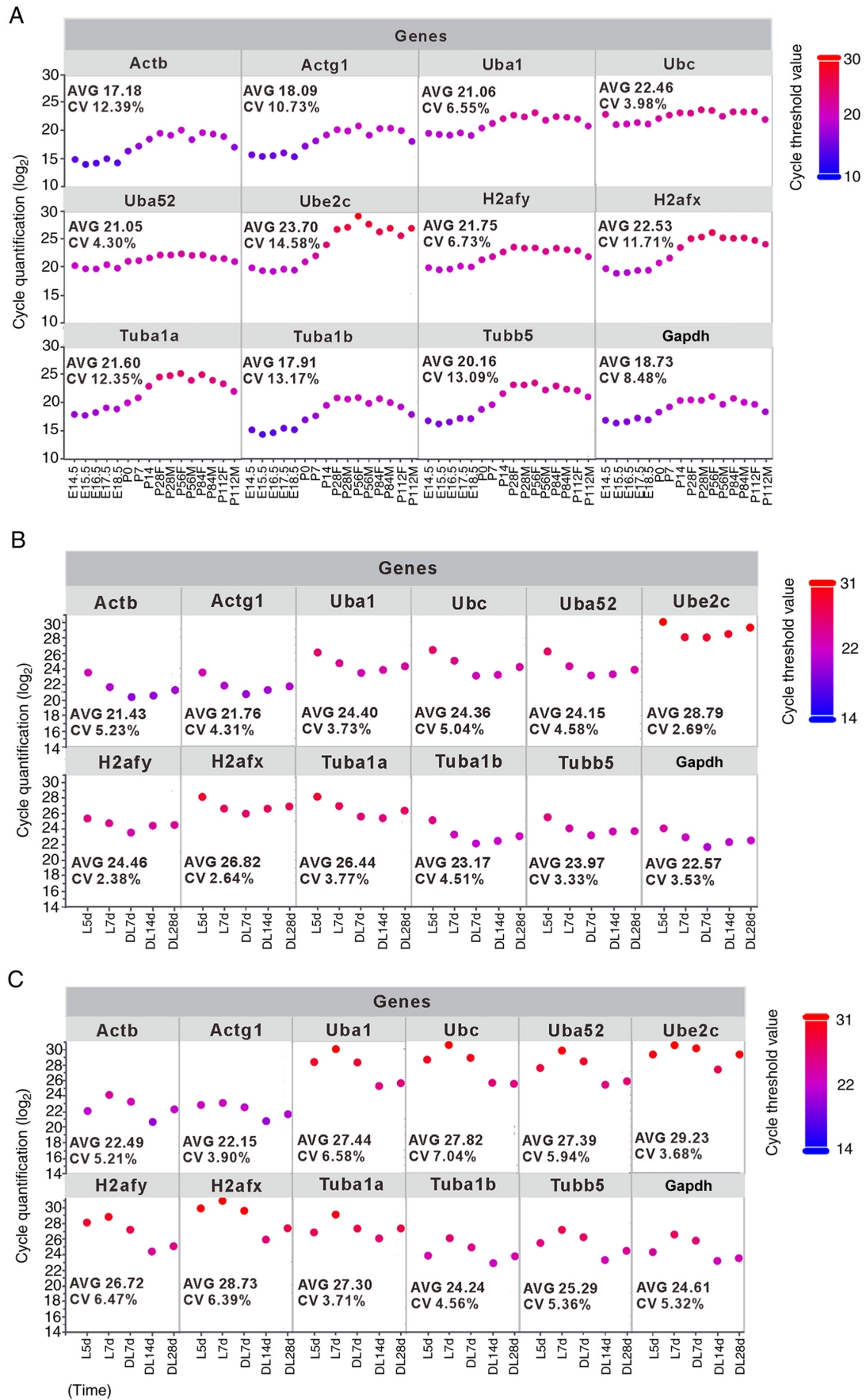
Figure 3. Expression variability of the 12 candidate reference genes among all tested samples during SMG development and regeneration. Raw expression was displayed as the quantification cycle (Cq) values detected using RT-qPCR and is presented as scatter plots. (A) SMG development group. Duct calculus-induced SMG regeneration model, including, (B) sham operation group, and (C) duct ligation/de-ligation group. Measurements were taken in triplicate for each time point sample. For visualization purposes, we have added a color bar representing the log2 values of cycle threshold. SMG, submandibular gland; AVG, average; M, male; F, female; E, embryonic day; P, post-natal; L, ligation; DL, de-ligation.

to the results from the development process. Furthermore, the CV values of the 12 candidate reference genes in all samples were as follows: 2.38% (*H2afy*), 2.64% (*H2afx*), 2.69% (*Ube2c*), 3.33% (*Tubb5*), 3.53% (*Gapdh*), 3.73% (*Uba1*), 3.77% (*Tuba1a*), 4.31% (*Actg1*), 4.51% (*Tuba1b*), 4.58% (*Uba52*), 5.04% (*Ubc*) and 5.23% (*Actb*) (Fig. 3B).

In the duct ligation/de-ligation group, the mean Cq values of the 12 candidate reference genes ranged from 22.15 (*Actg1*) to 29.23 (*Ube2c*) (Fig. 3C). The CV values of the 12 candidate reference genes in all samples were as follows: 3.68% (*Ube2c*), 3.71% (*Tuba1a*), 3.90% (*Actg1*), 4.56% (*Tuba1b*), 5.21% (*Actb*), 5.32% (*Gapdh*), 5.36% (*Tubb5*), 5.94% (*Uba52*), 6.39% (*H2afx*), 6.47% (*H2afy*), 6.58% (*Uba1*) and 7.04% (*Ubc*) (Fig. 3C).

Expression stability analysis of the 12 candidate reference genes in SMG development. To further evaluate the expression stability of the reference genes comprehensively in the SMG development state, gland samples were obtained from embryonic mice (E14.5, E15.5, E16.5, E17.5 and E18.5) and post-natal mice (P0, P7, P14, P28, P56, P84 and P112) for use in RT-qPCR. The geNorm, NormFinder, BestKeeper, ΔCq and RefFinder tools were then used. As demonstrated in Fig. 4, a Venn diagram was drawn to reveal the optimal reference genes. The top three recommended reference genes were different according to aforementioned software: *Uba1/H2afy > Gapdh > Actg1* with geNorm analysis, *Actg1 > Actb > Tuba1b* with NormFinder analysis, *Uba52 > Ubc > Uba1* with Bestkeeper analysis, and *Actg1/Actb > Tuba1b > H2afy* with ΔCq analysis. The least stable reference gene was *Ube2c*, as per all four statistical software (Fig. 4A and Table II). The most stable reference genes recommended by the four software were different; thus, the RefFinder software was employed to integrate the optimal reference gene. RefFinder analysis results indicated that *Actg1*, *H2afy* and *Uba1* are in the top three rankings and may be more stably expressed, whereas *Ube2c* was the least stable reference gene (Fig. 4E and Table II).

Expression stability analysis of the 12 candidate reference genes in SMG functional regeneration. To assess the expression stability of the 12 candidate reference genes in the SMG functional regeneration state, gland samples of 5-day ligation, 7-day ligation, 7-day de-ligation, 14-day delegation and 28-day de-ligation were selected for use in RT-qPCR. The ΔCq, M, SV and CV/SD values of the 12 candidate reference genes were then calculated using the four aforementioned statistical software. Finally, RefFinder software was used to integrate the aforementioned four statistical methods and calculate the recommended comprehensive ranking order for the expression stability of each candidate reference gene. As illustrated in Fig. 4B, the geNorm stability values of the top three genes calculated in the sham operation group: *Actb/Uba52 > Tuba1b > Actg1*. The NormFinder results revealed the expression stability of the top three reference genes listed from high to low: *Actg1 > Uba1 > Gapdh*. BestKeeper values showed the top three reference genes were *H2afy > H2afx > Tubb5*. The ΔCq values revealed that the top three reference genes were *Uba1*, *Actg1* and *Tuba1b*. The four types of evaluation methods designated *Ubc/Ube2c* as the least stable gene (Table II). The integrated analysis through RefFinder also indicated
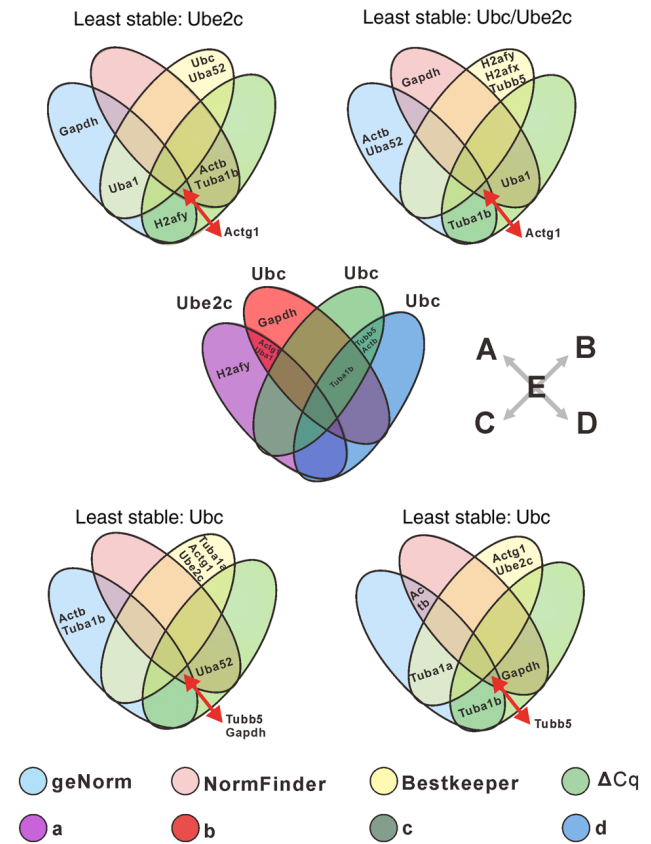

Figure 4. Comparison of the optimal reference genes using different software and experimental conditions. The Venn diagram compares the top three most suited reference genes. (A) SMG development group. Duct calculus-induced SMG regeneration model including the (B) sham operation group, (C) duct ligation/de-ligation group, and (D) ligation/de-ligation model combining sham operation and duct ligation/de-ligation group. (E) RefFinder software provided an overall comprehensive ranking under different experimental conditions; 'a' refers to the SMG development group, 'b' refers to the sham operation group, 'c' refers to the duct ligation/de-ligation group, and 'd' refers to the ligation/de-ligation model combining sham operation and duct ligation/de-ligation group. SMG, submandibular gland.

that the stability for the best three genes was *Actg1> Uba1 > Gapdh/Tuba1b*. On the other hand, the least stable gene was *Ubc* (Fig. 4E and Table II).

In the duct ligation/de-ligation group, the geNorm values indicated the order of the top three genes calculated for expression stability to be *Actb/Tuba1b > Tubb5 > Gapdh*. The NormFinder results revealed the expression stability of the top three reference genes was *Tubb5 > Uba52 > Gapdh*. The BestKeeper values revealed the top three reference genes to be *Tuba1a > Actg1 > Ube2c*. The ΔCq values revealed that the top three reference genes were *Tubb5*, *Uba52* and *Gapdh*. At the same time, the four-evaluation method analyses revealed that *Ubc* was also the least stable gene in the duct ligation/de-ligation group (Fig. 4C and Table II). Similarly, the ranks of the 12 most stable candidate reference genes were obtained from the above four software analyses and showed a slight difference. RefFinder analysis results indicated the stability of the top three genes to be ranked as *Tubb5 > Tuba1b > Actb*, and the *Ubc* gene was the least stable one (Fig. 4E and Table II).

The stability reference genes were also analyzed in the ligation/de-ligation model combining sham operation and duct ligation/de-ligation group. The geNorm values revealed that

Table II. Ranking of the 12 reference genes under multiple conditions according to five different types of software.

Group	Rank	geNorm Gene	geNorm Stability	NormFinder Gene	NormFinder Stability	BestKeeper Gene	BestKeeper SD	BestKeeper CV	ΔCq Gene	ΔCq SD	RefFinder Gene	RefFinder Stability
Development group	1	Uba1	0.26	Actg1	0.086	Uba52	0.78	3.70	Actg1	0.87	Actg1	2.21
	2	H2afy	0.26	Actb	0.117	Ubc	0.79	3.51	Actb	0.87	H2afy	2.99
	3	Gapdh	0.29	Tuba1b	0.293	Uba1	1.25	5.95	Tuba1b	0.93	Uba1	3.22
	4	Actg1	0.44	Gapdh	0.374	H2afy	1.30	5.98	H2afy	0.94	Actb	3.44
	5	Actb	0.50	H2afy	0.376	Gapdh	1.44	7.72	Gapdh	0.95	Gapdh	4.16
	6	Tuba1b	0.59	Uba1	0.466	Actg1	1.74	9.65	Uba1	0.99	Tuba1b	4.56
	7	Tubb5	0.70	Tubb5	0.505	Actb	1.90	11.09	Tubb5	1.05	Uba52	5.62
	8	Tuba1a	0.75	H2afx	0.557	Tuba1b	2.14	11.93	Tuba1a	1.10	Ubc	7.18
	9	H2afx	0.79	Tuba1a	0.559	Tubb5	2.44	12.10	H2afx	1.12	Tubb5	7.45
	10	Uba52	0.89	Uba52	0.845	Tuba1a	2.45	11.35	Uba52	1.34	Tuba1a	8.71
	11	Ubc	0.97	Ubc	0.977	H2afx	2.49	11.06	Ubc	1.49	H2afx	9.19
	12	Ube2c	1.13	Ube2c	1.293	Ube2c	3.23	13.62	Ube2c	1.93	Ube2c	12.00
Sham operation group	1	Actb	0.10	Actg1	0.030	H2afy	0.45	1.82	Uba1	0.30	Actg1	2.51
	2	Uba52	0.10	Uba1	0.053	H2afx	0.54	2.00	Actg1	0.31	Uba1	2.89
	3	Tuba1b	0.14	Gapdh	0.114	Tubb5	0.62	2.60	Tuba1b	0.33	Gapdh	4.12
	4	Actg1	0.18	Tuba1b	0.117	Gapdh	0.64	2.83	Gapdh	0.35	Tuba1b	4.12
	5	Uba1	0.20	Tubb5	0.134	Actg1	0.70	3.20	Tubb5	0.36	Actb	4.46
	6	Gapdh	0.23	Actb	0.185	Ube2c	0.71	2.46	Actb	0.37	Uba52	4.70
	7	Tubb5	0.25	Uba52	0.196	Uba1	0.73	3.01	Uba52	0.38	Tubb5	4.79
	8	Tuba1a	0.27	Tuba1a	0.212	Tuba1b	0.79	3.42	Tuba1a	0.41	H2afy	6.04
	9	Ubc	0.30	H2afx	0.224	Tuba1a	0.85	3.21	H2afx	0.43	H2afx	6.34
	10	H2afx	0.33	Ubc	0.321	Uba52	0.88	3.65	Ubc	0.51	Tuba1a	8.24
	11	H2afy	0.37	H2afy	0.333	Actb	0.89	4.15	H2afy	0.55	Ube2c	10.09
	12	Ube2c	0.41	Ube2c	0.405	Ubc	1.06	4.35	Ube2c	0.63	Ubc	10.19
Duct ligation/de-ligation group	1	Actb	0.29	Tubb5	0.148	Tuba1a	0.74	2.71	Tubb5	0.60	Tubb5	2.06
	2	Tuba1b	0.29	Uba52	0.263	Actg1	0.78	3.53	Uba52	0.69	Tuba1b	2.83
	3	Tubb5	0.40	Gapdh	0.278	Ube2c	0.81	2.76	Gapdh	0.71	Actb	3.34
	4	Gapdh	0.41	Actb	0.300	Tuba1b	0.96	3.96	Tuba1b	0.72	Gapdh	3.98
	5	Ube2c	0.45	Ube2c	0.327	Actb	0.97	4.33	Actb	0.73	Uba52	4.00
	6	Tuba1a	0.50	Tuba1b	0.329	Tubb5	1.16	4.60	Uba1	0.78	Tuba1a	5.19
	7	Actg1	0.55	Uba1	0.372	Gapdh	1.21	4.90	Ube2c	0.80	Ube2c	5.21
	8	Uba52	0.61	Actg1	0.414	Uba52	1.43	5.21	Actg1	0.85	Actg1	5.47
	9	Uba1	0.68	H2afx	0.420	H2afy	1.60	5.99	H2afx	0.85	Uba1	7.54
	10	H2afx	0.73	H2afy	0.449	Uba1	1.66	6.04	H2afy	0.86	H2afx	9.72

Table II. Continued.

| Group	Rank	geNorm		NormFinder		BestKeeper			ΔCq		RefFinder	
		Gene	Stability	Gene	Stability	Gene	SD	CV	Gene	SD	Gene	Stability
	11	H2afy	0.76	Tuba1a	0.508	H2afx	1.69	5.88	Tuba1a	0.92	H2afy	9.97
	12	Ubc	0.79	Ubc	0.508	Ubc	1.81	6.49	Ubc	0.94	Ubc	12.00
Combining sham operation and duct ligation/de-ligation group	1	Actb	0.23	Tubb5	0.182	Actg1	0.81	3.69	Tubb5	0.73	Tubb5	2.21
	2	Tuba1b	0.23	Gapdh	0.268	Ube2c	0.83	2.86	Gapdh	0.79	Tuba1b	2.63
	3	Tuba1a	0.33	Actb	0.332	Tuba1a	0.87	3.25	Tuba1b	0.80	Actb	3.16
	4	Tubb5	0.41	Tuba1b	0.360	Tuba1b	1.00	4.20	Actb	0.82	Gapdh	3.74
	5	Actg1	0.50	H2afx	0.381	Actb	1.09	4.96	H2afx	0.86	Actg1	4.49
	6	Ube2c	0.55	Uba52	0.408	Tubb5	1.14	4.64	H2afy	0.92	Tuba1a	4.58
	7	Gapdh	0.61	H2afy	0.432	Gapdh	1.21	5.14	Tuba1a	0.96	H2afx	5.73
	8	H2afx	0.69	Actg1	0.453	H2afy	1.48	5.77	Uba1	0.99	Ube2c	6.17
	9	H2afy	0.75	Uba1	0.462	H2afx	1.48	5.34	Actg1	1.02	H2afy	7.14
	10	Uba1	0.83	Ube2c	0.482	Uba1	1.76	6.79	Uba52	1.04	Uba1	8.94
	11	Uba52	0.88	Tuba1a	0.540	Uba52	1.78	6.91	Ube2c	1.07	Uba52	10.49
	12	Ubc	0.94	Ubc	0.636	Ubc	2.00	7.65	Ubc	1.23	Ubc	12.00
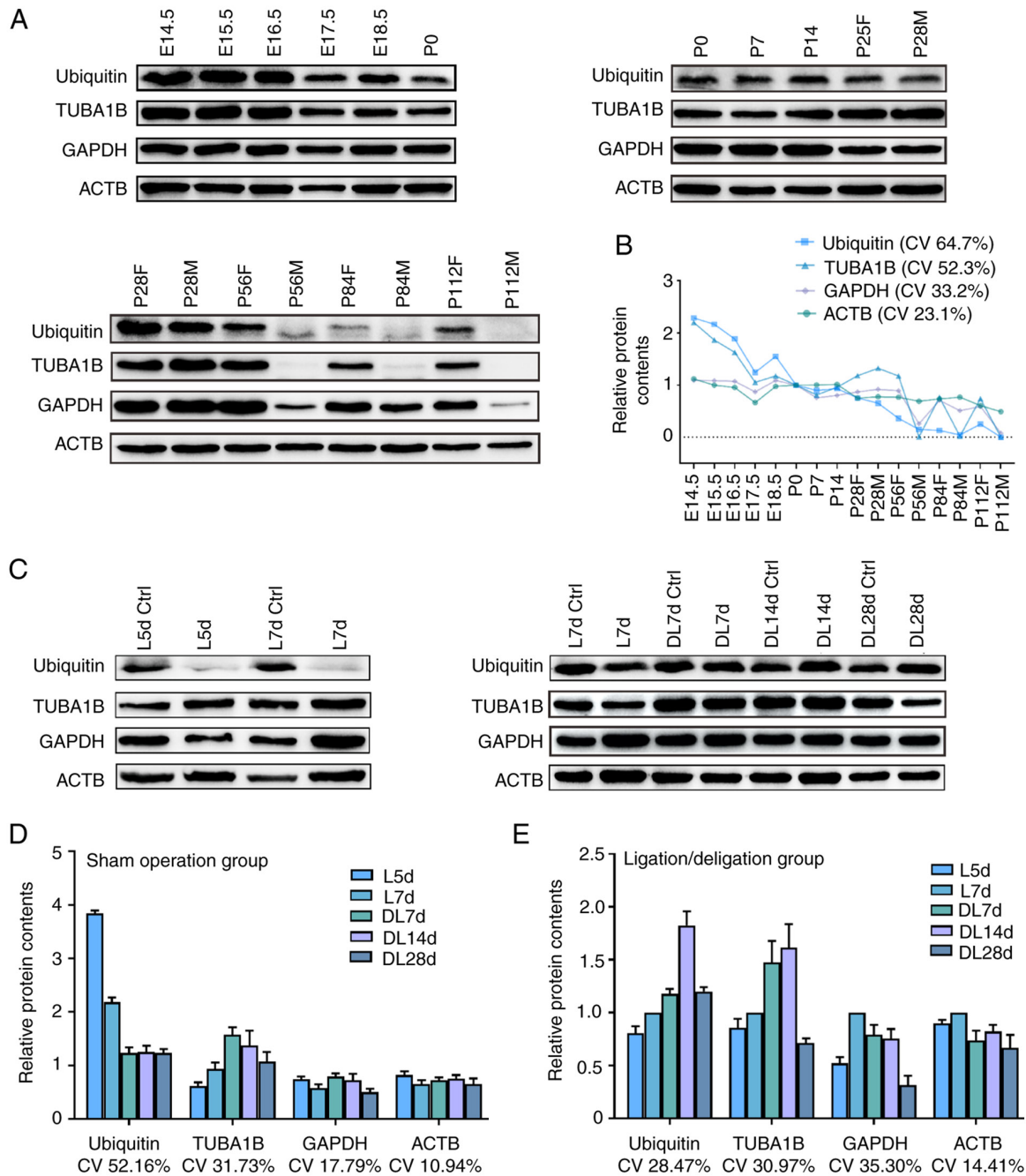
Figure 5. Validation of loading controls for western blot analysis throughout SMG development and regeneration. Representative western blots of ubiquitin, TUBA1B, GAPDH and ACTB were shown in (A) for distinct SMG developmental stages and (C) for duct calculus-induced SMG regeneration stages. Densitometric analysis and CV of ubiquitin, TUBA1B, GAPDH and ACTB are shown in (B) for SMG developmental stages, (D) sham operation group and (E) duct ligation/de-ligation group. In order to exclude the influence of exposure intensity, exposure time and other factors. The intensity of the protein bands for the lane loaded with duplicate samples was normalized to 1, such as P0, P28M, P28F, L7d ctrl, L7d. 'E', 'P', 'F', 'M', 'L' and 'DL' refer to embryo, post-natal, female, male, ligation and de-ligation, respectively. The experiment was repeated three times. CV, coefficient of variation; d, day; SMG, submandibular gland.

the top three genes calculated for expression stability were *Actb*/*Tuba1b* > *Tuba1a* > *Tubb5*. The NormFinder results revealed the top three reference genes, listed from high to low, as follows: *Tubb5* > *Gapdh* > *Actb*. The BestKeeper values revealed the top three reference genes were *Actg1* > *Ube2c* > *Tuba1a*. The ΔCq values revealed that the top three reference genes were *Tubb5*, *Gapdh* and *Tuba1b*. *Ubc* was designated as the least stable gene by the four algorithms mentioned above, while the most stable gene was disunified (Fig. 4D and Table II). The RefFinder results indicated the three most stable

genes to be *Tubb5* > *Tuba1b* > *Actb*, while the least stable gene was indicated to be *Ubc* (Fig. 4E and Table II).

Validation of loading control for western blot analysis. To further verify the stable reference gene in SMG development and functional regeneration stage, western blot analysis was performed to assess the expression of the represented protein. As shown in Fig. 5A and B, an evident variation in ubiquitin protein expression during the SMG development stage with a CV of 64.7%. Similarly, TUBA1B protein expression exhibited
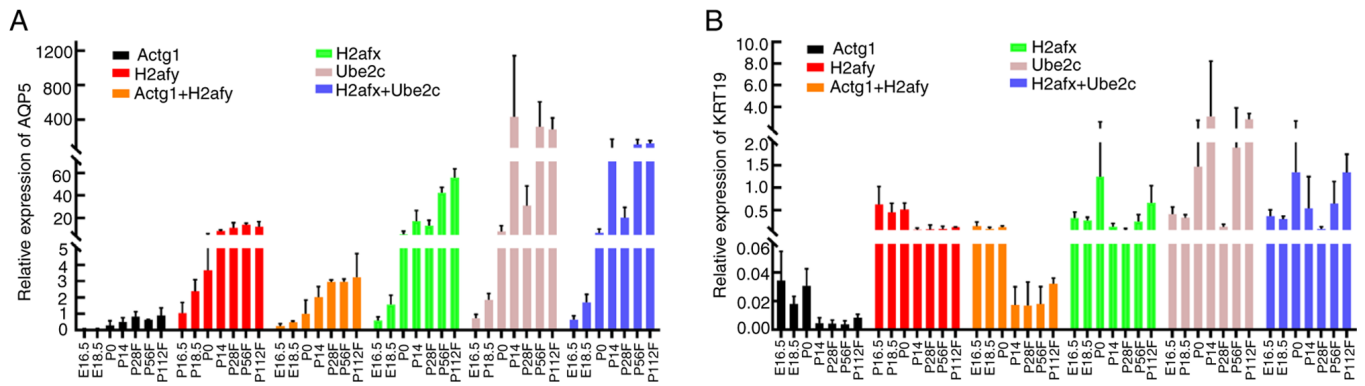
Figure 6. Relative expression patterns of the (A) *AQP5* gene and (B) *KRT19* gene under submandibular gland development. The most stable reference genes (Actg1 and H2afy) and unstable genes (H2afx and Ube2c) were selected for normalization of the qPCR data. Relative expression values are represented as mean ± standard deviation of three replicates. AQP5, aquaporin 5; KRT19, keratin 19; M, male; F, female; E, embryonic; P, post-natal.

an obvious variation with a CV of 52.3%. The GAPDH protein level variation (CV) value was 33.2%. Compared with ubiquitin, TUBA1B and GAPDH, the protein expression of ACTB was the least variable, with a CV of 23.1%. Furthermore, it was found that the expression of ACTB protein was relatively stable, particularly from P28 to P112, while that of the other three proteins varied greatly (Table SII). In brief, these results revealed that the expression level of ACTB was the most reliable loading control in western blot analysis, which was consistent with the results of RT-qPCR.

Subsequently, the present study analyzed the protein expression of ACTB, GAPDH, ubiquitin and TUBA1B in the SMG functional regeneration stage. As shown in Fig. 5C-E, the protein expression of ACTB, GAPDH and TUBA1B was slightly variable, with a CV of 10.94, 17.79 and 31.73%, respectively, in the sham operation group. The protein expression of ubiquitin exhibited an evident variation with a CV of 52.16%. In the ligation/de-ligation group, the protein expression of ACTB, ubiquitin, TUBA1B and GAPDH was slightly variable, with a CV of 14.41, 28.47, 30.97 and 35.30%, respectively. The results of the statistical analysis of the reference genes at different time periods are presented in Table SIII. Taken together, these results demonstrated that the protein expression level of ACTB in the SMG functional regeneration stage was the most appropriate loading control for western blot analysis.

Validation of selected reference genes. To assess the reliability of the selected reference gene, the relative expression levels of the target genes, *AQP5* and *KRT19*, were quantified in SMG developmental stages using RT-qPCR. The primer specificity of *AQP5* and *KRT19* was verified as described for the reference genes (Table I). The two most stable reference genes (*Actg1* and *H2afy*) and the two least stable reference genes (*H2afx* and *Ube2c*) identified using RefFinder software were used either alone or in combination to normalize the expression levels of *AQP5* and *KRT19* (Fig. 6).

Regardless of normalization by *Actg1* or *H2afy*, alone or in combination, similar expression patterns of *AQP5* were obtained. The expression level for *AQP5* mRNA was markedly increased from the embryonic stage (E16.5) to the post-natal stage (P112F), with the highest expression level observed at the P112F stage. However, the expression patterns of *AQP5*

differed when using *H2afx* or *Ube2c* independently or in combination as reference genes for normalization. The highest expression level of *AQP5* appeared at the P112F stage using either *H2afx* or in combination with *H2afx* as the reference gene for normalization, as well as at the P14 stage using Ube2c for normalization, while its expression level significantly decreased at the P28F stage using the two least stable reference genes for normalization data (Fig. 6A).

Similarly, the *KRT19* expression patterns were relatively the same when using *Actg1* or *H2afy*, alone or in combination, for normalization. The *KRT19* mRNA expression level peaked at around E16.5 and decreased after birth. However, when using *H2afx* or *Ube2c* independently or in combination as reference genes for normalization, it was found that the highest expression level of *KRT19* appeared at the P0 stage (Fig. 6B). Taken together, these results demonstrate that the selection of a suitable reference gene is crucial for the accurate normalization of qPCR data.

Discussion

As the main salivary gland in mammals, the SMG has been verified as a classical model for studying development and regeneration (35). However, the lack of reliable reference genes for normalized target gene expression may impede understanding of the underlying biology and molecular mechanisms. The present study investigated the expression stability of putative candidate reference genes during mouse SMG development and regeneration of superior reference genes.

The development model of the embryonic period in the SMG is a consecutive process that includes branching morphogenesis, lumen formation and mature acinar differentiation. Studies have indicated that the functional maturity of SMG is achieved after birth; for example, the differentiation of granular convoluted tubes begins at P7, the number of tubes increases around two weeks after birth, and the tubes finally mature at 4-6 weeks after birth (36,37). To comprehensively monitor the expression of reference genes throughout the developmental period, the present study collected samples at 12 time points from the embryo (E14.5, E15.5, E16.5, E17.5 and E18.5) to the post-natal stage (P0, P7, P14, P28, P56, P84 and P112), which involves gland branching, lumen formation,

acinar differentiation, gland maturation, sexual maturity and adulthood in mice. At the same time, the expression of reference genes was detected in different regenerative stages of the SMG following the duct ligation/de-ligation of the SMG model. The main secretory duct ligation/de-ligation of the SMG is a common model in the research of regeneration, accompanied by periodic changes associated with atrophy and the apoptosis of acinar epithelial cells, the proliferation of duct cells and differentiation of acini to restore secretion function (4,10). Furthermore, studies have confirmed that the regeneration of acinar epithelial cells reoccurred during 5-day and 7-day duct ligation (10). Pro-acinar cells were observed after 7-day de-ligation, and the number of mature acinar cells then increased after 14-day de-ligation. Finally, the structure and function of the gland were restored in the 28-day de-ligation samples. Thus, in the present study, five stages of SMG regeneration (5-day ligation, 7-day ligation, 7-day de-ligation, 14-day de-ligation and 28-day de-ligation) were used, following which the expression of the reference genes was representatively assessed. Moreover, H&E staining and AB/PAS staining were performed to confirm the successful establishment of the ligation/de-ligation model (Figs. S2 and S3). In brief, the present study comprehensively examined the stability of reference genes at different time points during the development and regeneration of SMG, covering a wide range of time points, which can provide a good reference for subsequent glandular studies.

As is known, SYBR-Green RT-qPCR is the preferred technique to quantify gene expression levels with high specificity, speed, accuracy, reproducibility, simplicity and sensitivity (38-40). However, experimental errors can be introduced due to RNA quality, DNA contamination, gene copy numbers, PCR amplification efficiency and the reverse transcription efficiency of test samples (41,42). Thus, to reduce these experimental errors, a stable reference gene is required to standardize target gene expression.

Reference genes are less affected by environmental factors, are widely detected in almost all tissues and are stably expressed in various stages within organisms. Common reference genes or nucleotide sequences include *Actb*, *Gapdh*, small ribosomal subunit (*18S*), ribosomal RNA (*rRNA*) and *Ubc*. However, it has been found that the transcriptional levels of these reference genes change as per different stages of the cell cycle, differences in tissues and differences in experimental conditions (17). Deindl *et al* (43) reported the mRNA level of *Actb* to be significantly upregulated during the first 24 h of collateral artery growth in a rabbit femoral artery ligation model. Furthermore, Suzuki *et al* (44) indicated the pitfalls of using 'classical' reference genes, such as *Actb* and *Gapdh*. Consequently, over the past two decades, a large number of researchers have paid attention to the stability studies of reference genes. However, due to technical advancements, particularly the rapid development of bioinformatics, the selection of reference genes is becoming increasingly global and systematic. Therefore, the present study selected a total of 12 candidate reference genes, namely, *Tuba1a*, *Tuba1b*, *Tubb5*, *H2afy*, *H2afx*, *Actb*, *Actg1*, *Ubc*, *Uba1*, *Uba52*, *Ube2c* and *Gapdh*, based on RNA-Seq data. Compared with SMG rat studies reported as early as 2008 (45), the present study used a more statistical method along with basic global data from

RNA-Seq to conduct a systematic analysis of reference genes during SMG development and regeneration, which provided new guidelines for the selection of reference genes, while studying the mouse SMG.

The Cq values obtained using RT-qPCR provide a simple and convenient assessment to pre-emptively provide a rough estimation for the stability of gene expression. In the present study, according to the Cq value, it was found that *Actb* was abundantly expressed in the SMG development group and sham operation group, and *Actg1* was the most expressed in the duct ligation/de-ligation group, while *Ube2c* was the least expressed in all groups. The aberrant expression of reference genes leads to intricate evaluation based on Cq values. Thus, sophisticated mathematical software (geNorm, NormFinder, BestKeeper, ΔCq and RefFinder) was used to assess reference gene stability. However, our results showed that the suitable reference genes analyzed by geNorm, NormFinder, BestKeeper, and ΔCq software were not consistent. In previous studies (46,47), the results have indicated this variation to partly be due to the different assumptions and algorithm models of each software (48,49). It was found that the rankings by NormFinder and ΔCq were similar, yet different from those assigned by geNorm and BestKeeper. This was also reported in a previous study by Herath *et al* (50). Therefore, RefFinder, a web-based tool, was used to comprehensively evaluate the stability of the reference genes. The RefFinder results suggested the most stable reference gene to be *Actg1* in SMG developmental stage and in the sham operation group. Combining sham operation and duct ligation/de-ligation group, the most stable reference gene was *Tubb5*, the expression of which is involved in the synthesis of microtubule components and its family members. The *Ube2c* and *Ubc* genes, the products of which participate in protein kinase activation, DNA repair, and chromatin dynamics, have been exploited as reference genes for a long time. Both *Ube2c* and *Ubc* were calculated to be the least stable reference gene, as ranked using geNorm, NormFinder, BestKeeper, ΔCq and RefFinder software.

To further confirm the reliability of loading controls, the present study investigated reference protein expression levels in SMG development and regeneration using western blot analysis. Based on the RT-qPCR results, the protein levels of the products of the most stable reference genes, ACTB and TUBA1B, in addition to those of the two classical candidates, ubiquitin and GAPDH, were quantified. Western blot analysis revealed the protein expression level of β-actin/g-actin to be more stable across all groups, compared to the expression pattern exhibited by classical reference proteins such as ubiquitin, TUBA1B and GAPDH. Although the primers designed to target *Actb* and *Actg1* were specific, it should be noted that the specific antibody was used to detect the protein expression level of ACTB and ACTG1 separately due to slight differences in the amino acid sequence. Additionally, the antibody against TUBA1B has the same target amino acid sequence as TUBB5; thus, more specific antibodies are required to discriminate ideal reference proteins in future research.

To validate the reliability of the selected reference genes, the expression patterns of *AQP5* and *KRT19* under the SMG developmental stage were evaluated. It is well known that AQP5 is a key water channel and KRT19 is a cytoskeletal protein; both play important roles in salivary gland

function (51,52). Accordingly, the two most stable genes (*Actg1* and *H2afy*) and the two least stable genes (*H2afx* and *Ube2c*), as recommended using RefFinder software under the SMG developmental stage, were used to verify target gene expression patterns. The results revealed that when the most stable genes (*Actg1*, *H2afy*, and *Actg1* + *H2afy*) were used to normalize the expression levels of *AQP5* and *KRT19*, similar expression patterns were obtained. For example, the highest expression level of *AQP5* and *KRT19* appeared at the P112 and P56 stage, respectively. By contrast, when the least stable genes (*H2afx*, *Ube2c*, and *H2afx* + *Ube2c*) were used to calibrate the expression data, the expression patterns and transcript levels of *AQP5* and *KRT19* varied notably. As per the results, *AQP5* had the highest expression level at the P112 stage, using *H2afx* and *H2afx* + *Ube2c* genes for normalization, and at the P14 stage, using Ube2c for normalization. *AQP5* expression patterns exhibited a rapid decrease at the P28F stage when using *H2afx*, *Ube2c*, and *H2afx* + *Ube2c* genes for normalization. Furthermore, *KRT19* appeared to have the highest expression level at the P0 stage when using *H2afx*, *Ube2c*, and *H2afx* + *Ube2c* genes for normalization. Previous studies have demonstrated that using an unstable reference gene generates biases and may lead to reduced accuracy or misinterpreted results in the RT-qPCR assay (53-55). These results are in accordance with such findings. Consequently, the use of reliable reference genes for normalization is a preliminary requirement for obtaining accurate relative gene expression levels.

In conclusion, the present study evaluated the stability of 12 candidate reference genes during SMG development and regeneration using five statistical algorithms (BestKeeper, NormFinder, geNorm, ΔCq and RefFinder). *Actg1* was identified as the most reliable reference gene during the SMG developmental stage, and *Tubb5* was recommended as the most stable reference gene for the SMG regenerative stage, whereas the least stable reference genes were *Ubc* and *Ubc2e*. The results obtained in the present study provide useful information for the generation of accurate RT-qPCR data in gene expression studies of SMG development and regeneration.

Acknowledgements

Not applicable.

Funding

Availability of data and materials

The datasets used and/or analyzed during the current study are available from the corresponding author on reasonable request. The raw data for this study have been deposited in the SRA database (accession no. PRJNA856858; to be release on June 30, 2023).

Authors' contributions

WL, TZ and DY designed the experiments. LH contributed to the writing of the manuscript. LH, HL, QC, WL and TZ performed the experiments. LH, HL and QC analyzed the data. LH and HL confirm the authenticity of all the raw data. All authors have read and approved the final manuscript.

Ethics approval and consent to participate

All animal experiments were approved by the Ethics Committee of Chongqing Medical University College and Use Committee (approval no. 2021062). The Guidelines for the Ethical Review of Laboratory Animal Welfare (GB/T35892-2018, China) were applied in the experiments. The study was conducted according to the guidelines of ARRIVE and AVMA euthanasia 2020, and followed the '3R' principles for the treatment of experimental animals: Replacement, reduction and refinement.

Patient consent for publication

Not applicable.

Competing interests

The authors declare that they have no competing interests.

References

1. Proctor GB: The physiology of salivary secretion. Periodontol 2000 70: 11-25, 2016.
2. Emmerson E and Knox SM: Salivary gland stem cells: A review of development, regeneration and cancer. Genesis 56: e23211, 2018.
3. Miletich I: Introduction to salivary glands: Structure, function and embryonic development. Front Oral Biol 14: 1-20, 2010.
4. Hosoi K, Yao C, Hasegawa T, Yoshimura H and Akamatsu T: Dynamics of salivary gland AQP5 under normal and pathologic conditions. Int J Mol Sci 21: 1182, 2020.
5. Gresik EW, Chung KW, Barka T and Schenkein I: Immunocytochemical localization of nerve growth factor, submandibular glands of Tfm/Y mice. Am J Anat 158: 247-250, 1980.
6. Schenck K, Schreurs O, Hayashi K and Helgeland K: The role of nerve growth factor (NGF) and its precursor forms in oral wound healing. Int J Mol Sci 18: 386, 2017.
7. Suzuki A, Ogata K and Iwata J: Cell signaling regulation in salivary gland development. Cell Mol Life Sci 78: 3299-3315, 2021.
8. Wang Y, Dong J, Li D, Lai L, Siwko S, Li Y and Liu M: Lgr4 regulates mammary gland development and stem cell activity through the pluripotency transcription factor Sox2. Stem Cells 31: 1921-1931, 2013.
9. Patel N, Sharpe PT and Miletich I: Coordination of epithelial branching and salivary gland lumen formation by Wnt and FGF signals. Dev Biol 358: 156-167, 2011.
10. Hishida S, Ozaki N, Honda T, Shigetomi T, Ueda M, Hibi H and Sugiura Y: Atrophy of submandibular gland by the duct ligation and a blockade of SP receptor in rats. Nagoya J Med Sci 78: 215-227, 2016.
11. Woods LT, Camden JM, El-Sayed FG, Khalafalla MG, Petris MJ, Erb L and Weisman GA: Increased expression of TGF-β signaling components in a mouse model of fibrosis induced by submandibular gland duct ligation. PLoS One 10: e0123641, 2015.
12. Tran ON, Wang H, Dean DD, Chen XD and Yeh CK: Stem cell-based restoration of salivary gland function. In: A Roadmap to Nonhematopoietic Stem Cell-Based Therapeutics: From the Bench to the Clinic. Elsevier, pp345-66, 2019.

13. Shimizu O, Yasumitsu T, Shiratsuchi H, Oka S, Watanabe T, Saito T and Yonehara Y: Immunolocalization of FGF-2, -7, -8, -10 and FGFR-1-4 during regeneration of the rat submandibular gland. J Mol Histol 46: 421-429, 2015.
14. Baum BJ, Alevizos I, Chiorini JA, Cotrim AP and Zheng C: Advances in salivary gland gene therapy - oral and systemic implications. Expert Opin Biol Ther 15: 1443-1454, 2015.
15. González CR, Amer MA, Vitullo AD, González-Calvar SI and Vacas MI: Immunolocalization of the TGFB1 system in submandibular gland fibrosis after experimental periodontitis in rats. Acta Odontol Latinoam 29: 138-143, 2016.
16. Hai B, Zhao Q, Qin L, Rangaraj D, Gutti VR and Liu F: Rescue effects and underlying mechanisms of intragland shh gene delivery on irradiation-induced hyposalivation. Hum Gene Ther 27: 390-399, 2016.
17. Wang B, Duan H, Chong P, Su S, Shan L, Yi D, Wang L and Li Y: Systematic selection and validation of suitable reference genes for quantitative real-time PCR normalization studies of gene expression in Nitraria tangutorum. Sci Rep 10: 15891, 2020.
18. Yang NY, Mukaibo T, Kurtz I and Melvin JE: The apical Na⁺-HCO₃⁻ cotransporter Slc4a7 (NBCn1) does not contribute to bicarbonate transport by mouse salivary gland ducts. J Cell Physiol 10: 1002, 2019.
19. Tanaka J, Ogawa `M, Hojo H, Kawashima Y, Mabuchi Y, Hata K, Nakamura S, Yasuhara R, Takamatsu K, Irié T, et al: Generation of orthotopically functional salivary gland from embryonic stem cells. Nat Commun 9: 4216, 2018.
20. Zhang Y, Fan J, Sun J, Francis F and Chen J: Transcriptome analysis of the salivary glands of the grain aphid, Sitobion avenae. Sci Rep 7: 15911, 2017.
21. Ruan W and Lai M: Actin, a reliable marker of internal control? Clin Chim Acta 385: 1-5, 2007.
22. Bunnell TM, Burbach BJ, Shimizu Y and Ervasti JM: β-actin specifically controls cell growth, migration, and the G-actin pool. Mol Biol Cell 22: 4047-4058, 2011.
23. Guo C, Liu S, Wang J, Sun MZ and Greenaway FT: ACTB in cancer. Clin Chim Acta 417: 39-44, 2013.
24. Binarová P and Tuszynski J: Tubulin: Structure, functions and roles in disease. Cells 8: 1294, 2019.
25. Nicholls C, Li H and Liu JP: GAPDH: A common enzyme with uncommon functions. Clin Exp Pharmacol Physiol 39: 674-679, 2012.
26. Seidler NW: Basic biology of GAPDH. Adv Exp Med Biol 985: 1-36, 2013.
27. Zhang JY, Zhang F, Hong CQ, Giuliano AE, Cui XJ, Zhou GJ, Zhang GJ and Cui YK: Critical protein GAPDH and its regulatory mechanisms in cancer cells. Cancer Biol Med 12: 10-22, 2015.
28. Chen ZJ and Sun LJ: Nonproteolytic functions of ubiquitin in cell signaling. Mol Cell 33: 275-286, 2009.
29. Livak KJ and Schmittgen TD: Analysis of relative gene expression data using real-time quantitative PCR and the 2(-Delta Delta C(T)) method. Methods 25: 402-408, 2001.
30. Ramakers C, Ruijter JM, Deprez RH and Moorman AF: Assumption-free analysis of quantitative real-time polymerase chain reaction (PCR) data. Neurosci Lett 339: 62-66, 2003.
31. Vandesompele J, De Preter K, Pattyn F, Poppe B, Van Roy N, De Paepe A and Speleman F: Accurate normalization of real-time quantitative RT-PCR data by geometric averaging of multiple internal control genes. Genome Biol 3: RESEARCH0034, 2002.
32. Andersen CL, Jensen JL and Ørntoft TF: Normalization of real-time quantitative reverse transcription-PCR data: A model-based variance estimation approach to identify genes suited for normalization, applied to bladder and colon cancer data sets. Cancer Res 64: 5245-5250, 2004.
33. Pfaffl MW, Tichopad A, Prgomet C and Neuvians TP: Determination of stable housekeeping genes, differentially regulated target genes and sample integrity: BestKeeper-excel-based tool using pair-wise correlations. Biotechnol Lett 26: 509-515, 2004.
34. Xie F, Xiao P, Chen D, Xu L and Zhang B: miRDeepFinder: A miRNA analysis tool for deep sequencing of plant small RNAs. Plant Mol Biol 31: 1007, 2012.
35. Chatzeli L, Teshima THN, Hajihosseini MK, Gaete M, Proctor GB and Tucker AS: Comparing development and regeneration in the submandibular gland highlights distinct mechanisms. J Anat 238: 1371-1385, 2021.
36. Gresik EW: Postnatal developmental changes in submandibular glands of rats and mice. J Histochem Cytochem 28: 860-870, 1980.
37. Srinivasan R and Chang WW: The development of the granular convoluted duct in the rat submandibular gland. Anat Rec 182: 29-39, 1975.
38. Borkowska P, Zielińska A, Paul-Samojedny M, Stojko R and Kowalski J: Evaluation of reference genes for quantitative real-time PCR in Wharton's Jelly-derived mesenchymal stem cells after lentiviral transduction and differentiation. Mol Biol Rep 47: 1107-1115, 2020.
39. Li Z, Lu H, He Z, Wang C, Wang Y and Ji X: Selection of appropriate reference genes for quantitative real-time reverse transcription PCR in Betula platyphylla under salt and osmotic stress conditions. PLoS One 14: e0225926, 2019.
40. Wu Y, Tian Q, Huang W, Liu J, Xia X, Yang X and Mou H: Identification and evaluation of reference genes for quantitative real-time PCR analysis in Passiflora edulis under stem rot condition. Mol Biol Rep 47: 2951-2962, 2020.
41. Zhu J, Zhang L, Li W, Han S, Yang W and Qi L: Reference gene selection for quantitative real-time PCR normalization in Caragana intermedia under different abiotic stress conditions. PLoS one 8: e53196, 2013.
42. Li J, Han X, Wang C, Qi W, Zhang W, Tang L and Zhao X: Validation of suitable reference genes for RT-qPCR data in achyranthes bidentata blume under different experimental conditions. Front Plant Sci 8: 776, 2017.
43. Deindl E, Boengler K, van Royen N and Schaper W: Differential expression of GAPDH and beta3-actin in growing collateral arteries. Mol Cell Biochem 236: 139-146, 2002.
44. Suzuki T, Higgins PJ and Crawford DR: Control selection for RNA quantitation. Biotechniques 29: 332-337, 2000.
45. Silver N, Cotroneo E, Proctor G, Osailan S, Paterson KL and Carpenter GH: Selection of housekeeping genes for gene expression studies in the adult rat submandibular gland under normal, inflamed, atrophic and regenerative states. BMC Mol Biol 9: 64, 2008.
46. Chen L, Zhong HY, Kuang JF, Li JG, Lu WJ and Chen JY: Validation of reference genes for RT-qPCR studies of gene expression in banana fruit under different experimental conditions. Planta 234: 377-390, 2011.
47. Cheng Y, Bian W, Pang X, Yu J, Ahammed GJ, Zhou G, Wang R, Ruan M, Li Z, Ye Q, et al: Genome-wide identification and evaluation of reference genes for quantitative RT-PCR analysis during tomato fruit development. Front Plant Sci 8: 1440, 2017.
48. Costa J, Saraiva K, Morais V, Oliveira J, Sousa D, Melo D, Morais J and Vasconcelos I: Reference gene identification for real-time PCR analyses in soybean leaves under fungus (Cercospora kikuchii) infection and treatments with salicylic and jasmonic acids. Australasian Plant Pathology 45: 191-199, 2016.
49. Zhang Y, Peng X, Liu Y, Li Y, Luo Y, Wang X and Tang H: Evaluation of suitable reference genes for qRT-PCR normalization in strawberry (Fragaria x ananassa) under different experimental conditions. BMC Mol Biol 19: 8, 2018.
50. Herath S, Dai H, Erlich J, Au AY, Taylor K, Succar L and Endre ZH: Selection and validation of reference genes for normalisation of gene expression in ischaemic and toxicological studies in kidney disease. PLoS One 15: e0233109, 2020.
51. Matsuzaki T, Suzuki T, Koyama H, Tanaka S and Takata K: Aquaporin-5 (AQP5), a water channel protein, in the rat salivary and lacrimal glands: Immunolocalization and effect of secretory stimulation. Cell Tissue Res 295: 513-521, 1999.
52. Hauser BR and Hoffman MP: Regulatory mechanisms driving salivary gland organogenesis. Curr Top Dev Biol 115: 111-130, 2015.
53. Li C, Hu L, Wang X, Liu H, Tian H and Wang J: Selection of reliable reference genes for gene expression analysis in seeds at different developmental stages and across various tissues in Paeonia ostii. Mol Biol Rep 46: 6003-6011, 2019.
54. Dos Santos CP, da Cruz Saraiva KD, Batista MC, Germano TA and Costa JH: Identification and evaluation of reference genes for reliable normalization of real-time quantitative PCR data in acerola fruit, leaf, and flower. Mol Biol Rep 47: 953-965, 2020.
55. Wang X, Wu Z, Bao W, Hu H, Chen M, Chai T and Wang H: Identification and evaluation of reference genes for quantitative real-time PCR analysis in Polygonum cuspidatum based on transcriptome data. BMC Plant Biol 19: 498, 2019.